Hybrid Wavelet-Based Algorithms for Fast Harmonic Identification

Ileana-Diana V.D. Nicolae*, Petre-Marian T. Nicolae, Marian-Ştefan P.M. Nicolae****

**Department of Computers and Information Technology*
(e-mail:nicolae_ileana@software.ucv.ro)
***Department of Electrical Engineering, Power Systems and Aeronautics*
(e-mail:pnicolae@elth.ucv.ro , snicolae@elth.ucv.ro)
University of Craiova, Decebal Blv. No. 107

Abstract: The paper deals with the logic, implementation and testing of original algorithms that provide a fast identification of harmonic disturbances when they pollute a monitored signal which in stationary state is characterized by periodical medium distortions. Unlike Fourier-based techniques, the identification requires for the harmonic identification only a small number of samples, corresponding to three quarters from a period of the monitored signal. The algorithms use the details vectors corresponding to the first 9 levels from a decomposition tree generated with 3 different original hybrid wavelet-based algorithms (relying on filters of length 4, 6 and 8). We identified the "key-features" of the details vectors and combined them such as to form "harmonic fingerprints", afterward stored in a partitioned matrix (*MHF*) along with the harmonic orders responsible for their generation. Using *MHF*, 30000 tests considering randomly generated polluting harmonics demonstrated that the mean run-time consumed for the harmonic order identification was reduced by a factor in the range (3.44...4.54). Percents under 0.15% of "absent fingerprint" situations were noticed, the algorithms being provided with intelligent additional execution branches to deal with them. The modest additional memory requirements and good run-time related performances, along with their relative simple implementation recommend the algorithms as valuable tools in real-time applications for power quality monitoring and fault identification.

Keywords: Search methods, Signal processing algorithms, Fault detection and identification, Frequency signal analysis, Harmonics, Wavelet analysis.

1. INTRODUCTION

Identification of harmonic related disturbances has been representing a permanent concern of professionals all over the globe, a common approach being the utilization of wavelet-based techniques.

For example, using wavelets, Chan, W.L., So, A.T.P. and Lai, L.L. (2000) proved that each type of current waveform polluted with power harmonics can be represented well by a normalized energy vector. Such vectors can be used for harmonics signature recognition, the corresponding system performing well in tandem with an artificial neural network (NN).

Similarly, a comparative study was made by Srivastava, S., Gupta, J.R.P. and Gupta, M. (2009), relative to neural NN-s related training algorithms. The studied NN was trained to extract important features from the input current waveform to uniquely identify various types of devices using their distinct harmonic signatures. The particle swarm optimization (PSO), genetic algorithm, gradient descent (GD) and respectively a hybrid of PSO&GD were analyzed, the last one proving to be superior.

Remarkable results obtained with a wavelet-genetic algorithm-neural network-based hybrid model relative to accurate prediction of short-term load forecast were communicated by Lai, L.L. and Zhou, L. (2010).

We have published recently some of the results we have obtained in the direction of fast identification of harmonic disturbances using wavelet-based techniques implemented by means of the dedicated Matlab function dwt with the mother function 'db3' (Nicolae, I.D. and Nicolae M.S. (2011) , Nicolae, I.D. and Nicolae, P.M. (2012a)). The harmonic identification related results were impressive, but our most recently studies revealed some drawbacks of the Matlab function dwt related to the evaluation of power quality indices and fault detection (Nicolae, I.D. and Nicolae P.M. (2012b)).

We have therefore conceived an original class of hybrid wavelet-based algorithms characterised by fast reconstruction properties, good abilities in fault detection and evaluation of power quality indices (Nicolae, I.D., et al. (2012 c)). The next step was to reveal the algorithms abilities related to the fast identification of harmonic disturbances, as described below.

2. PRELIMINARY EVALUATIONS

2.1. Wavelet algorithms

The analyzed class of hybrid wavelets algorithms used for the determination of approximation/detail vectors when performing a Discrete Wavelet Transform (DWT)

decomposition of a signal s with a filter of length l (belonging to the set {4,6,8}) can be described by (Nicolae, I.D., et al. (2012 c)):

$$a_i = s(i)\cdot h_0 + s(i+1)\cdot h_1 + ... + s(i+l-1)\cdot h_{i+l-1} + s(i+l-1)\cdot h_{l-1}$$
$$d_i = s(i)\cdot g_0 + s(i+1)\cdot g_1 + ... + s(i+l-1)\cdot g_{i+l-1} + s(i+l-1)\cdot g_{l-1}. \quad (1)$$

where for the first decomposition level the vector *s* contains the signal's discrete values, *a* and *d* denote the approximation/detail vectors, obtained when *s* is decomposed using the low-pass filter $h=[h_0\ h_1\ \ldots h_{l-1}]$ having the values from Table 1 and a high-pass filter $g=[g_0\ g_1\ \ldots g_{l-1}]$, constructed with $g_i = (-1)^i h_{l-1-i}, i = 0...l-1$ (Van Fleet, P. (2009), Percival, D. and Walden, A, (2006)).

Table 1. Coefficients of low pass filters approximated to 2 decimal places

Filter length	h_0	h_1	h_2	h_3	h_4	h_5	h_6	h_7
4	0.48	0.84	0.22	-0.12	-	-	-	-
6	0.33	0.81	0.46	-0.13	-0.08	0.03	-	-
8	0.23	0.71	0.63	-0.03	-0.18	0.03	0.03	-0.01

For stationary waves, we considered that the missing values beyond the right edge (*n*) of the currently analyzed data segment are equal to those from the left edge. So: $s(n+i)=s(i)$, with $i=1\ldots l-2$. Beginning with the 2-nd decomposition level, the role of *s* is played by the approximations from the previous level.

2.2. Preliminary evaluations in stationary regime

The monitored signal (a current from the supplying network - Fig. 1) has distortions and is typical for stationary regimes in power systems. The details corresponding to the first level of decomposition have almost negligible values, with maximum values not exceeding 0.5 A . For decomposition levels of higher orders the details become more significant, denoting the presence of regular distortions of harmonic nature (generated by low-order harmonics) in stationary regime,

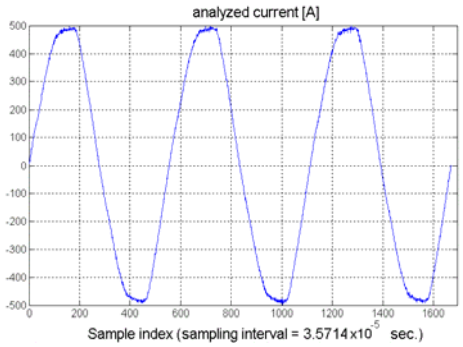

Fig. 1. Signal submitted to preliminary evaluations

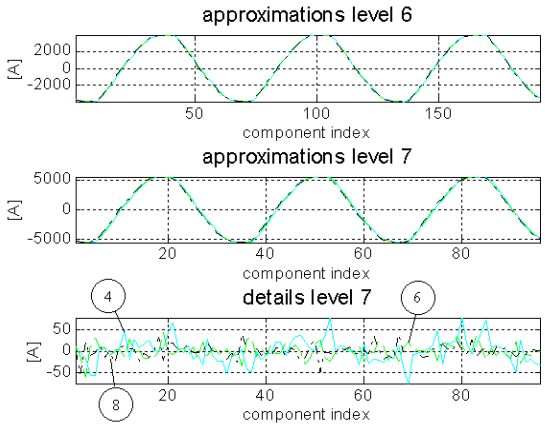

Fig. 2. Stationary. Decomposition of the 6-th level.

as depicted by Fig.2, where the circles mention the filter's length (Nicolae, I.D et al. (2012 c)). As expected from the underlying algorithms and values of filters' coefficients, the maximum and minimum values recorded by details within a period if generated by shorter filters are higher in absolute values while more local peaks can be noticed when longer filters are used (Fig. 3).

For each filter length and decomposition level, the details' maximum absolute value for the median period (*MA1*) was evaluated in stationary state. Another important parameter that must be evaluated in stationary regime is the maximum absolute value for all three periods (*MA2),*

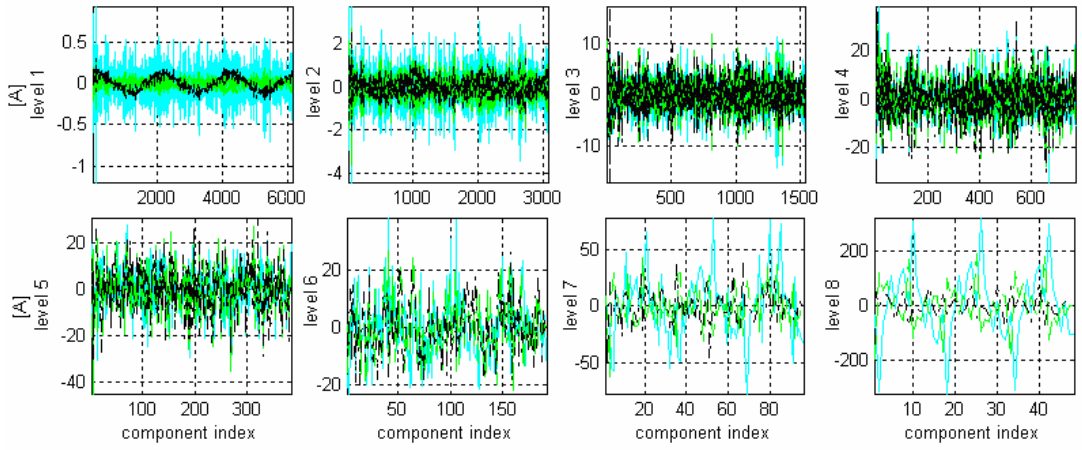

Fig. 3. Stationary. Details for decomposition levels with orders within the range 1...8, generated by all filters (cyan – filter of length 4; green – filter of length 6; black – filter of length 8) .

always higher than *MA1* owing to a moderate "edge effect" exhibited by all filters.

The ratios *MA2/MA1* represent the decomposition levels' intrinsic sensitivities to fault detection, because a fault occurred near the signal edges affected by the edge effect can be shadowed if the details' deviations do not overcame the value of *MA2*.

2.3. Decomposition levels' sensitivities to harmonic pollution

To test the abilities of all filters relative to detection and evaluation of harmonic pollutions, firstly a signal with a nature of harmonic pollution was superposed over the data segment in stationary regime, containing the samples with indexes in the range [*l*/4...*l*/2], where *l* represents the length of the currently analyzed segment, as in Fig. 4.

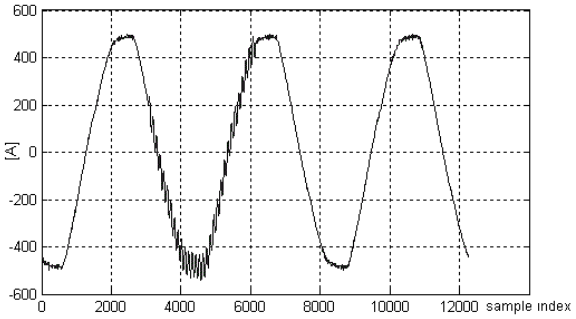

Fig. 4. Monitored signal affected by the harmonic of order 40 with amplitude 50 and phase difference 0.

The harmonics amplitude was set to 50A whilst the harmonic orders (*HO*) were varied from 3 to 40. The phase difference (*Ph*), calculated between the sine waveform used as harmonic pollution and the polluted signal at the moment when pollution started was also varied from -π to π with steps of π/6.

The levels' sensitivities were calculated with respect to the *HO* and phase difference respectively. As *Ph* influences the level's sensitivity, two waveforms (one with all maximum values, the other with all minimum values) were represented for each level and filter length. The sensitivities on the first 4 levels, increasing with the *HO* in an almost linear manner, were found to be too small to provide reliable information on faults, unlike those for decomposition levels higher than 5 (Fig. 5) (Nicolae, I.D et al. (2012 c)).

3. DETERMINATION OF THE KEY-FEATURES FOR THE HARMONIC IDENTIFICATION

The experience that we gained during our previous researches in the area ((Nicolae, I.D. and Nicolae M.S. (2011), Nicolae, I.D. and Nicolae, P.M. (2012a)) made us start with a study on the differences between two sets of vectors (now calculated with our original hybrid wavelet-based algorithms) (Fig.6):
- the details affected by the harmonic pollution;
- the details determined in the stationary regimes.

Considering the levels sensitivities versus *HO*-s presented in Section 2, the analysis was made only for the levels 5...9. Figs. 6 and 7 depict partial representations of the vectors corresponding to these differences, when the pollution was made by signals with *HO*-s from the extreme values of the range of interest (3 and 40 respectively), but with identical phase differences and amplitudes (*Ph* =0, amplitude 50).

Another characteristic (also revealed in the case when dwt from Matlab was employed) is the similarity of shapes when different harmonic amplitudes were used as test data. Fig. 8 depicts results obtained with a filter of length 8, polluting *HO* = 40, *Ph* of π-π/750.

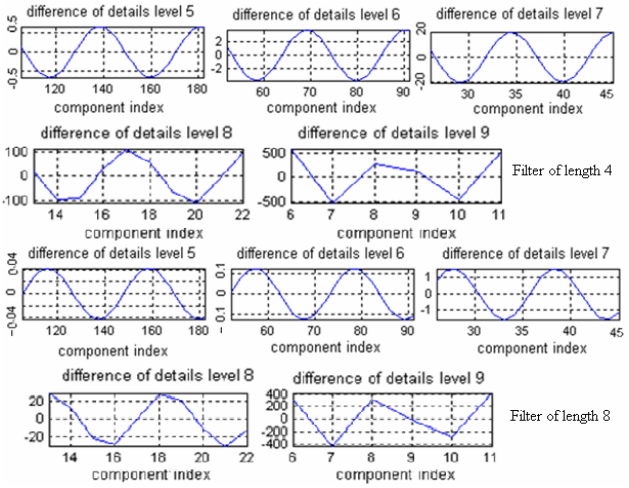

Fig. 6. Partial representation of the difference between details for levels 5...9. Up – filter of length 4 and down - filter of length 8. Harmonic pollution with order 3.

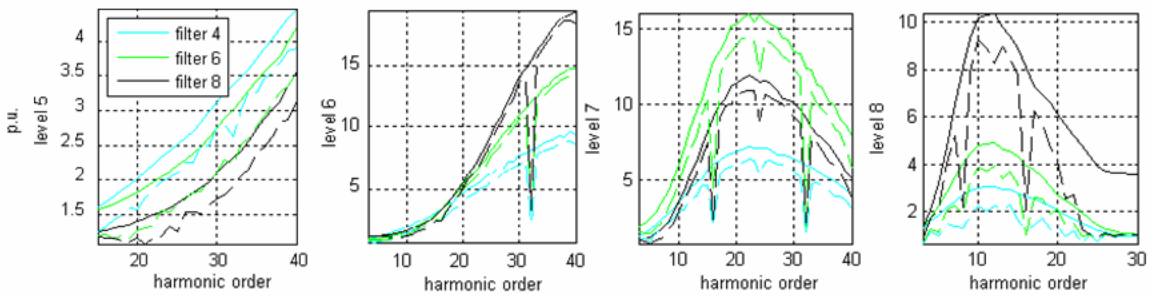

Fig. 5. Sensitivities at fault versus harmonic order (continuous / dashed line for maximum / minimum values relative to phase differences varying from –π to π in steps of π/6).

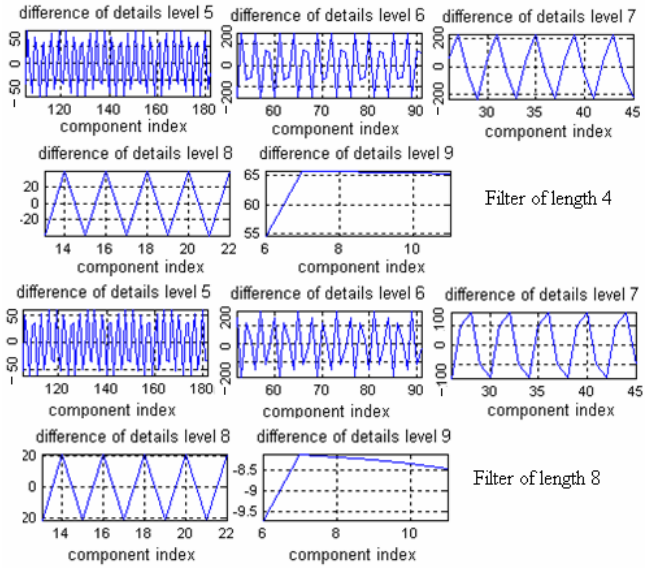

Fig. 7. Partial representation of the difference between details for levels 8 and 9. Up – filter of length 4 and down - filter of length 8. Harmonic pollution with order 40.

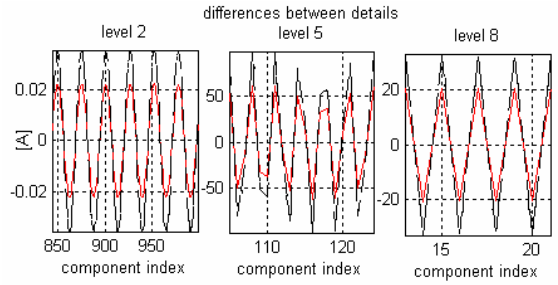

Fig. 8. Partial representation of the difference between details (harmonically polluted – stationary) for levels 2, 5 and 8. Smaller values (red) – harmonic amplitude =50, higher values (black) - harmonic amplitude = 80.

As expected, the difference vectors present more oscillations for higher *HO*-s. The amplitudes of harmonics do not affect the number of oscillations (*NO*) and therefore, for a certain filter, *NO* on each level is affected by only 2 parameters: the harmonic order and the phase difference. These features recommend *NO*-s as reliable candidates for the harmonic pollution identification.

4. ALGORITHMS USED FOR HARMONIC IDENTIFICATION.

4.1. Data structures

To generate an appropriate number of "harmonic fingerprints", polluting harmonic signals were generated considering an amplitude of 50A , harmonic orders from 3 to 40 and *Ph* covering the range [–π...π) with a constant step of π/750.

A harmonic signal generated in this way was overlapped over the stationary signal for a discrete interval corresponding to the samples from the range [*l*/4...*l*/2+2048], where *l* corresponds to 3 periods of the stationary signal and consequently a non-stationary signal was obtained, as in Fig.9. For the first 9 levels of

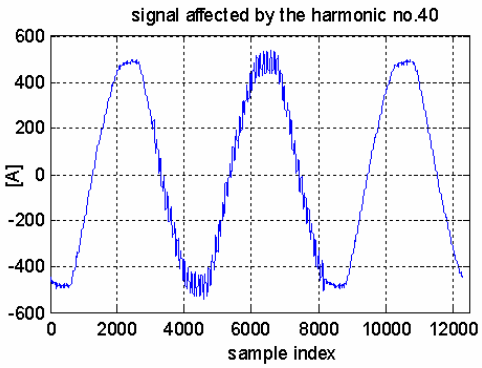

Fig. 9. Nonstationary signal used to construct the search structures, affected by the harmonic no. 40, *Ph* = 0.

decomposition, vectors containing the differences (details for nonstationary – details for stationary) were calculated, generically described as

diff_level_i=details_nonstationary_level_i- details_stationary_level_i,

with *i*=1...9.

For each *HO*, the distinct combinations obtained by gathering the NO–s corresponding to each *diff_level_i* (*i*=5...9) (calculated when all phase differences were considered), were stored as possible „harmonic fingerprints" (*HF*) in specific data structures (Fig. 10).

Filter of length 4		
harmonic no. 3	harmonic no. 16	harmonic no. 40
5 5 5 5 5 5 5 5 5 6 4 5 5 5 5 4 4 5 5 5 4 4 5 6 5 4 4 4 5 5	... 24 25 25 0 1 24 25 25 0 7 24 25 25 0 0 25 25 25 0 1 25 25 24 0 2 25 25 24 0 0 25 25 24 0 3 ...	60 37 12 13 0 61 37 12 13 0 61 37 12 13 1 61 37 12 13 2 61 36 12 13 0 61 36 13 13 0 61 37 13 13 0 61 37 13 12 0
Filter of length 6		
harmonic no. 3	harmonic no. 16	harmonic no. 40
... 4 5 13 5 6 4 5 13 5 5 5 5 13 5 5 5 5 14 5 5 6 5 14 5 5 6 6 14 5 5 6 6 12 5 5 ...	... 24 25 25 0 5 25 25 25 0 5 25 24 25 0 5 24 24 25 0 5 24 24 25 2 5 24 24 25 6 5 24 24 25 7 5 ...	... 60 37 13 13 0 60 37 13 11 0 60 37 13 9 0 ... 61 37 12 13 2 61 37 12 13 4 61 37 12 13 5 61 37 12 13 3 ...
Filter of length 8		
harmonic no. 3	harmonic no. 16	harmonic no. 40
... 6 6 4 5 5 6 4 4 5 5 4 4 4 5 5 4 4 5 5 5 5 4 5 5 5 5 5 5 5 5 ...	... 25 24 25 0 3 25 24 24 0 3 25 24 25 0 4 26 24 25 0 4 24 24 25 0 4 **24 24 25 0 1** ...	60 37 13 13 1 60 37 13 13 0 61 37 13 13 0 .. 61 36 12 13 0 61 37 13 13 1 61 37 13 13 3

Fig. 10. Examples of harmonic fingerprints.

For example when the filter of length 8 was used to perform the wavelet decomposition and a harmonic polluting signal with the harmonic order 16 was overlapped over the stationary signal as described above, for certain phase differences 24 oscillations were detected in *diff_level_5* and in *diff_level_6*, 25 oscillations were detected in *diff_level_7* whilst *diff_level_7* oscillated only once and *diff_level_6* had no oscillations (as revealed by the bolded *HF* from Fig. 10).

For each distinct filter length a specific procedure was executed to check for duplicates and it was found that for a certain filter, each *HF* was generated by a single harmonic and therefore a certain *HF* can be used for the unambiguous identification of the *HO* of the polluting signal that generated it.

Fig. 11 presents the number of *HF* generated by each harmonic order when different filter lengths were used.

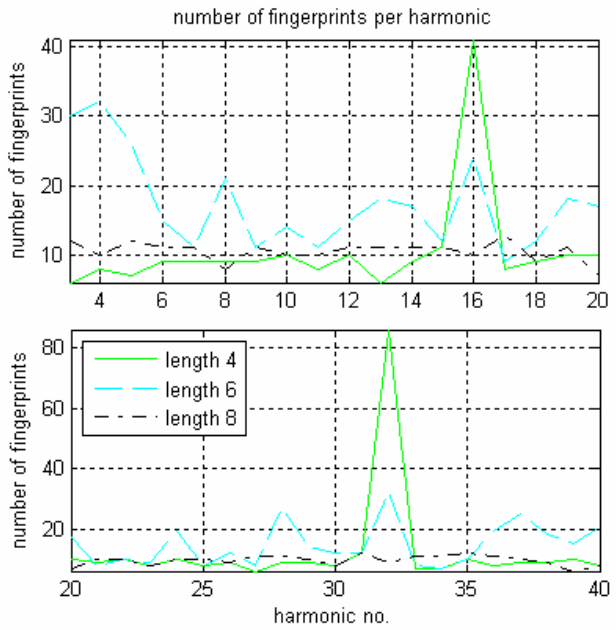

Fig. 11. Number of harmonic fingerprints versus harmonic order, for all filters.

More *HF*-s were generated for certain *HO* - s (e.g. 4, 8, 16, 32), proving that a small number of duplicates were found for them. It means that for these harmonics (we should call them "critical frequencies" *CF*) the *Ph* has a more significant influence, more individualized patterns being obtained in the shape of details . A previous Fourier analysis of the monitored signal in stationary regimes revealed that *CF*-s match to the most significant harmonics from its spectrum. The same set of frequencies is responsible for the irregularities noticed in the levels sensitivities versus harmonic orders from Fig. 5.

The next step was to gather for each distinct filter length all the *HF* - s within a single matrix (referred below as MHF_l, where *l* can be the filter length), still preserving the identification of the harmonic *h* that generated it by means of a dedicated additional column. MHF_4 has 441 rows, MHF_6 has 607 rows whilst MHF_8 has 385 rows.

An inspection of the above mentioned matrices reveals that the content of their first column can be used for their partitioning such as to refine the search and reduce the time required to find a specific row. Considering this, the next step was to sort every MHF_l in the ascending order of the values from its first column. Partitions were afterward determined inside every matrix, each of them containing all the rows for which the first column has the same values. A similar partitioning technique was used in (Ümit V. Çatalyürek (2008).

Fig. 12 depicts the first rows from MHF_4 . The horizontal lines emphasizes the partitions limits, the bolded values correspond to the harmonic order which generated the *HF* corresponding to that row and the italicized characters represent the values used for the partitioning.

4	4	5	5	5	**3**
4	4	5	6	5	**3**
4	4	4	5	5	**3**
4	5	5	5	5	**3**
5	5	5	5	5	**3**
5	5	5	5	6	**3**
6	6	7	6	7	**4**
6	6	6	6	7	**4**
6	6	6	7	7	**4**
6	6	7	7	7	**4**
6	6	7	7	6	**4**
6	7	7	6	7	**4**
6	7	7	7	7	**4**
7	7	7	7	7	**4**
			.....		

Fig. 12. Example of rows from MHF_4 .

Fig. 13 depicts the partitions sizes. Obviously smaller partition sizes mean smaller retrieval times. For this point of view, one expects to obtain the smallest average retrieval times relative to the search within partition for the filter of length 8, where the partitions sizes cannot contain more than 12 rows. This comes to fortunately balance somehow the longer times required for the determination of a specific harmonic fingerprint, as the time consumed for the determination of the detail vectors increases with the filter length.

The angular step considered when the matrices were built was small enough such as to provide a „hit ratio" higher than 99.9% for the tests described in the following

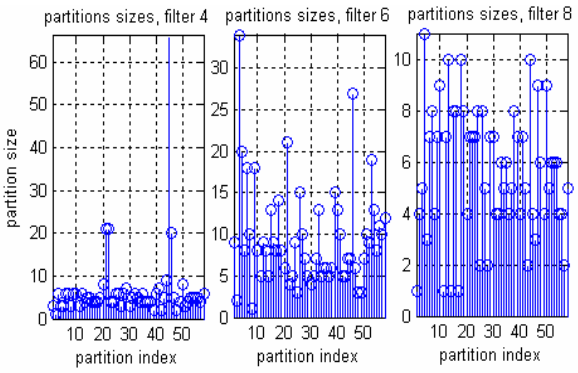

Fig. 13. Partition sizes.

section. Still, to provide the identification of any possible combination of harmonic pollution, a simple method was implemented and successfully used. This assumes:
- the estimation of the harmonic pollution as a difference: (stationary signal - nonstationary signal polluted with a specific harmonic h) ;
- the evaluation of the average number of samples (*ANS*) which correspond to one of its periods.

The procedure was run for every harmonic order within the range of interest [3...40] (Fig. 14) and the obtained *ANS* –s were stored in a dedicated array, with 37 rows, one for each harmonic order. As expected, the curve from Fig. 14 demonstrates a strict decreasing of the number of samples corresponding to a period from the polluting signal with the increasing of the harmonic order. As during the tests on some execution branches some estimated harmonic periods did not match exactly the central value determined during the "training stage" when the data structures were filled, high and low limits were also calculated and stored such as to provide larger limits and allow the *HO* identification.

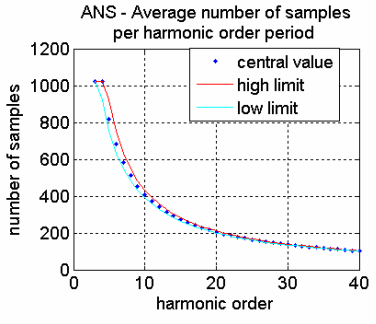

Fig. 14. Average number of samples per harmonic period.

Tests over 50000 of randomly generated harmonics revealed a 71.7% percent of harmonic orders directly identified using the central values from Fig. 14. The corresponding mismatching distribution is revealed by Fig. 15. Its analysis reveals maximum values not exceeding 6-7%. Their correlation to an overall mismatching ratio of around 28.3% results into the conclusion that no further run-time related improvement of the algorithm could be used in this direction.

4.2. Harmonics identification

Tests were made considering 2 sets of 30000 polluting signals of harmonic nature, randomly generated according to the following pattern:

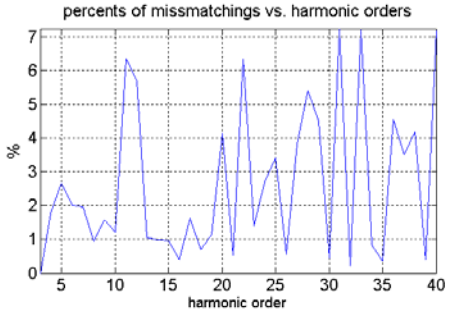

Fig. 15. Percents of *ANS* – related mismatching versus harmonic orders.

$$amplitude = rand() \cdot \max(I)/2;$$
$$phase\ \ difference = \pi / 750 * randi(1500) + rand() * 0.033;$$
$$h = randi(harm\_max) + 3,$$

where I represents the monitored signal, randi(x) generates randomly integer numbers within the range [0..x], rand() generates randomly real numbers within the range [0,1) and *harm_max* was set to 37 (to generate harmonic orders up to 40, which is the upper limit for harmonics under survey according to EU norms).

Within each test, wavelet decompositions up to the 9-th level were performed and the corresponding *HF* was built. Using an "interval halving" technique its first component was used to identify the corresponding partition from MH_l . A linear search (whose performances are improved because the rows within a partition follow an ascending sorting order with respect to the second column (Hitachi Co., 2007)) must be afterward performed to locate the harmonic fingerprint. A successful localization results into the harmonic order identification, as the searched harmonic order is stored in the last column from the located row. For cases of type "*HF* absent", the *ANS*-s must be used.

An analysis considering the "*HF* absent" cases generated on a 30000 tests basis for which the maximum harmonic order was set to 40 (Fig. 16) revealed a high percent of occurrences (50.13%) corresponding to 15040 cases for the filter of length 6. This percent is correlated to the highest rum time recorded during its employment and classifies it as unusable for this type of harmonic identification algorithm (the 23% percent of saved runtime does not justify the algorithm's additional memory requirements and implementation-related effort).

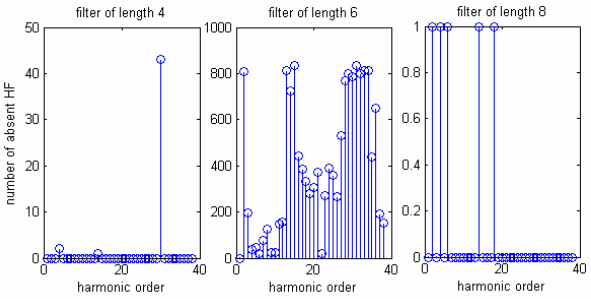

Fig. 16. Number of absent *HF*-s versus harmonic orders.

On the other hand, insignificant percents of "absent *HF*" were noticed for the other two filters: 0.15% occurrences for the filter of length 4 and 0.00017% for that of length 8 respectively. More details are presented below:
- 46 cases of "*HF* absent" for the filter of length 4 (from which 93.4% were generated by the 32-nd *HO*, 0.043% were generated by the 6-th *HO* whilst the remaining 0.021% were generated by the 16-th *HO*);
- 5 cases of "*HF* absent" for the filter of length 8, for the *HO*–s 4, 6, 8, 16 and 20 respectively.

Both the per-harmonic distribution of *HF*-s (Fig. 11) and respectively the levels sensitivity diagrams (Fig. 5) could have been used to anticipate this behavior, as the above mentioned *HO*-s belong mainly to the set of *CF*-s.

A solution to reduce the number of absent *HF*-s that are possible to be generated in the presence of the *CF*-s might be the calculation of more *HF*-s through the use of an angular step smaller than $\pi/750$, but the additionally generated *HF*-s should inflate the existing partitions, involving higher algorithm-related memory requirements. Finally this should slow down the harmonic-identification procedures instead of improving their efficiency. A more convenient solution should consist into an intelligent arrangement of the lines from the matrix storing the *ANS*-s. Placing the rows corresponding to the *CF*-s on this matrix's first positions (as they exhibited the greatest *HF* absent – associated probability) eliminates the risk of wasting runtime with sequential searches.

5. TESTS RESULTS

The mean runtimes required by tests are gathered by Table 2. For all tests, the harmonic orders were 100% correctly identified. The ratios (runtimes corresponding to the original algorithms) / (runtimes corresponding to the evaluation using only *ANS-s)* were smaller than 1 for all filters, as follows: for the filter of length 4 a ratio of 0.2857, for the filter of length 6 a ratio of 0.6015 and respectively for the filter of length 8 a ratio of 0.2236.

The "almost 0" value specified for the filters of length 4 and 8 for the "solving *HF* absent" action has a confusing meaning in this context, as the real mean runtime elapsed to solve the "*HF* absent" cases is slightly higher then that corresponding to the *HO* evaluation using only the *ANS* -s (as runtime is inevitably wasted trying to find a missing *HF*). The "almost zero" means that the average was made considering the total number of tests, an insignificant probability (mentioned in Section4) being related to the "*HF* absent" cases.

Table 2. Mean runtimes exhibited by harmonic identification algorithms

	Filter length		
Action/ Mean time [msec.]	4	6	8
Evaluation of *HF*	0.00936	0.00832	0.01040
Partition identification	0.00676	0.002080	0.001040
Search within partition	0.00780	0.004600	0.007280
Solving *HF* absent cases	almost 0	0.03536	almost 0
HO evaluation through original method (sum of the rows above)	0.02392	0.05036	0.01872
HO evaluation using only the *ANS* –s	0.08372	0.08372	0.08372

6. CONCLUSIONS

The class of original hybrid wavelet-based algorithms can be used for the fast identification of a polluting harmonic signal, with 2 major advantages over the use of Fast Fourier Transform:

- only a very small number of samples is required for analysis (3 quarters from a period of the monitored signal, starting from the moment when the pollution begins), so the identification procedure can start very soon after the harmonic pollution begins and corrective measures can be taken earlier;
- short-lasting (perhaps with intermittent features, only a limit of continuous 1.5 periods from the monitored signal being imposed to their presence) harmonic pollutions can be identified .

The original algorithms based on "harmonic fingerprints" provide significant runtime savings (by a ratio of 3.44 or 4.54, depending on which dwt filter is used) with the price of small additional memory requirements and acceptable programming effort.

Our future work will address the reducing of runtimes for the calculation of DWT decomposition vectors.

REFERENCES

Chan, W.L., So, A.T.P. and Lai, L.L., (2000), Wavelet feature vectors for neural network based harmonics load recognition, in *Proceedings of APSCOM-00,*, vol. 2, pp. 511 – 516

Hitachi Co. (2007) , Scalable Database Server, HiRDB Version 8 Description (Table matrix partitioning), available at *http://www.hitachi.co.jp/Prod/comp/soft1/manual/hirdben/v8/d635100e/W3510059.HTM*

Jensen, A., Cor-Harbo, A., (2001), *Ripples in Mathematics. The Discrete Wavelet Transform*, Springer Verlag.

Lai, L.L. and Zhou, L. (2010), Signal Processing for Improving Power Quality, in *Handbook of Power Systems II, Energy Syst.*, Springer Verlag, pp. 55-100.

Misiti, M., Y. Misiti, G. Oppenheim, J.-M. Poggi (2007), *Wavelets and their applications*, ISTE DSP Series.

Nicolae, I.D. and Nicolae M.S. (2011) , Using Wavelets to Define and Detect Harmonic Fingerprints in Non-Sinusoidal Waveforms, *Proceedings of SOFTCOM 2011*, 19-th International Conf. on Software Telecomm. and Computer Networks, SYM 2/III - 75923 – 1609.

Nicolae, I.D. and Nicolae, P.M. (2012a), Using wavelet transform for power systems, R*evue Roumaine de Sciences Techniques – Électrotechnique et Énergetique*, 57 (*2*), p. 172–182.

Nicolae, I.D. and Nicolae P.M. (2012b), Performances Evaluation of a Class of Original Discrete Wavelet Transform Based Hybrid Algorithms, *Proceedings of the International Conference on Harmonics and Quality of Power , ICHQP 2012*, pp.1-6.

Nicolae, I.D., Nicolae, P.M. and Popa, L.D. (2012 c) , *Abilities of a Class of Wavelet Hybrid Algorithms Related to Fault Detection in Power Systems,* under press for A*nnals of the University of Craiova, Electrical Engineering Series*, vol. 36 , 6 pages.

Percival, D. and Walden, A, (2006) *Wavelet Methods for Time Series Analysis*, , Cambridge University Press.

Srivastava, S., Gupta, J.R.P. and Gupta, M. (2009), PSO and neural-network based signature recognition for harmonic source identification, in *Proceedings of IEEE Conference TENCON 2009*, pp. 1-5

Van Fleet, P. (2009) Discrete Wavelet Transformations: *An Elemententary Approach with Applications*, Wiley-Interscience.